

SUPPLEMENTAL INFORMATION

TITLE: Impaired Reelin Dab1 signaling contributes to neuronal migration deficits of TSC

Tuberous Sclerosis Complex

Uk Yeol Moon^{1,2}, Jun Young Park^{1,2}, Raehee Park^{1,2}, Jennifer Y. Cho¹, Lucinda J. Hughes^{1,3}, James McKenna III⁶, Laura Goetzl^{1,4}, Seo-Hee Cho^{1,2}, Peter B. Crino^{1,5}, Michael J. Gambello⁶, Seonhee Kim^{1,2,*}

Running Title: mTOR and Reelin-Dab1 in neuronal migration

¹*Shriners Hospitals Pediatric Research Center*, ²*Department of Anatomy and Cell Biology*, ³*Graduate program of Biomedical Sciences* ⁴*Department of Obstetrics Gynecology and Reproductive Sciences* ⁵*Department of Neurology, Temple University School of Medicine, Philadelphia, PA, 19140*

⁶*Department of Human Genetics, Emory University, School of Medicine, Atlanta, GA, 30322*

SUPPLEMENTAL PROCEDURE (related to Experimental Procedure)

Antibody information for immunohistochemistry and Western blot: Primary antibodies, including Reelin (MAB5364, Millipore), Dab1 (B3, gift from Dr. Howell), GAPDH (sc-166574, Santa Cruz Biotechnology), Cul5 (sc-13014, Santa Cruz Biotechnology), Cux1(sc-13024, Santa Cruz Biotechnology), FoxP1(ab16645, Abcam), FoxP2(ab16046, Abcam), Ctip2 (ab28448, Abcam), BrdU (347580, BD bioscience), Tbr1 (Millipore), GFP (4B10), phospho-S6 (Ser240/244, #2215, Cell Signaling Technology), phospho-tyrosine(#9411, Cell Signaling Technology), phospho-Dab1 (Tyr220, #3327, Cell Signaling Technology), SFK(#2123, Cell Signaling Technology), and phospho-SFK (#6943, Cell Signaling Technology), were used for immunostaining or Western blot analysis. Primary antibodies were diluted in PBS with 5% goat serum for immunostaining or TBST with 5% skim milk for Western blot.

quantitative (q)PCR: Real-time PCR was performed using an Applied Biosystems StepOne™ and StepOnePlus™ Real-Time PCR system with LuminoCt® SYBR® Green qPCR ReadyMix™ (Sigma-Aldrich). Reactions were performed in a total volume of 20 µl which included 10 µl of 2XSYBR Green qPCR Ready Mix, 300nM of each primer (listed in Supplemental Table), and 1 µl of previously reverse-transcribed cDNA template. The thermocycler parameters were 95°C for 10 min, followed by 40 cycles of 95°C for 15 s and 60°C for 1 min. All reactions were performed in triplicate.

Quantification of neuronal positioning: Cortical areas from the pia to the lower end of intermediate zone were divided into 10 equal-sized bins and Cux1 immunopositive and GFP expressing cells in each bin were counted. The percentage of immune-positive or GFP expressing cells in each bin was then calculated for each section. We analyzed 3 nonconsecutive

sections taken from 3-5 WT- or CKO- electroporated mice. Student's t-test was applied to assess the statistical significance. $P < 0.05$ was regarded as statistically significant.

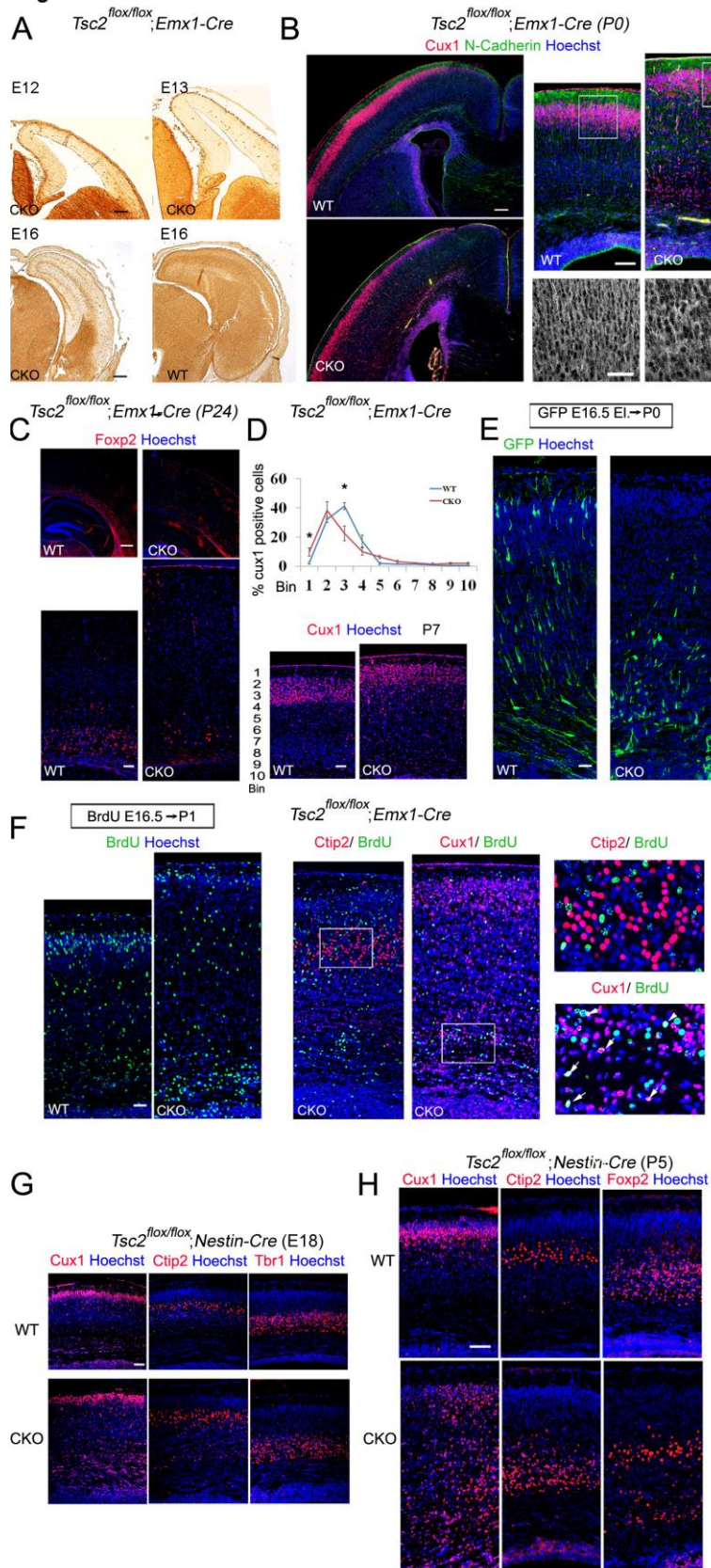
Leading process analysis: To analyze leading process complexity and length, we prepared thick sections using a vibratome. For vibratome sections, 4 % paraformaldehyde (PFA) fixed tissues were embedded in 10% gelatin and fixed again in 4 % PFA for 4 days, then sectioned at 200 μm using Leica VT1000s. Z-stack confocal images of vibratome sections spanning 50-100 μm were reconstructed into 3 dimensional images using Imaris (Bitplane), and the morphology of neurons whose leading process contacted the MZ was traced in detail. The length of leading processes was measured as the distance between branch point and soma using Imaris (Bitplane), and branch number was manually counted.

SUPPLEMENTAL TABLE

Primer sequences for PCR

Gene name	Forward	Reverse	Product size (bp)
Cul5 (RT-PCR)	GCACAGGCTCGTGTACTGA	TCGGGGTTGGAGCAAAGATT	350
Cul5 (Q-PCR)	TCC TCG TTT CCT TAC TGC AAG A	CAACCCCACTCCTTTTGGCT	103
Dab1	GTGAATGACATGCACGGTGT	ATCAGCTTGGCTTTGTACCG	263
Reelin	CTGGTCCCTACTCCACACTG	GCCAGAAAATCCTGGGTCAC	292
Socs7	TCAGTCGCCTGTTTCGCAC	GTTTCCTCCCCGTATCCAGC	153
18s rRNA	GAATAATGGAATAGGACCGCGG	GGAACTACGACGGTATCTGATC	216
β-actin (Q-PCR)	CTGAACCCTAAGGCCAACC	CCTGGATGGCTACGTACATG	85

Figure S1



SUPPLEMENTAL FIGURES

Figure S1. *Tsc2*-deficiency due to *Emx1*-Cre and *Nestin*-Cre shows neuronal migration defects and disrupted lamination (related to Figure 1)

(A) *Tsc2* protein is substantially reduced in the *Tsc2* CKO beginning at E12.5. (B) The soma size of *Cux1* positive cells outlined by N-cadherin immunostaining is increased in the *Tsc2* CKO compared to WT at P0. (C) Reduced number of *FoxP2*-positive layer 6 neurons in the *Tsc2* CKO at P24 compared to WT. (D) At P7, more *Cux1*-positive neurons are present in bin1 (MZ) and bin 3 in the CKO compared to WT. (E) *In utero* electroporation with pCAG-GFP at E16.5 demonstrates markedly delayed migration of *Tsc2* CKO neurons at P0 compared to WT. (F) Migration of neurons born on E16.5 (late-born) is severely delayed in the *Tsc2* CKO. BrdU-positive late-born neurons mainly populate the upper layer of cortical plate in WT, whereas BrdU-positive cells in *Tsc2* CKO are broadly distributed in cortical plate or accumulate in subventricular zone and ventricular zone. BrdU-positive cells in the lower cortex and IZ are *Cux1*-positive but not *Ctip2* positive. (G and H) Lamination defects in *Tsc2^{flox/flox}; Nestin-Cre* mice are demonstrated by layer-specific markers *Cux1* (layers 2-4), *Ctip2* (layer 5), *Tbr1* and *Foxp2* (layer 6) at E18.5 (G) and P5 (H). Many *Cux1*-positive neurons are ectopically located in the deeper cortical layers and *Ctip2*-positive neurons are widely dispersed in the *Tsc2^{flox/flox}; Nestin-Cre* mice compared to WT. Deeper layer neurons marked by *Tbr1* and *Foxp2* are less affected in the *Tsc2^{flox/flox}; Nestin-Cre* mice. Scale bar: 200 μm (B left and C top), 100 μm (A and D), 40 μm (B top, E, F and G), 20 μm (B bottom and C enlarged).

Figure S2

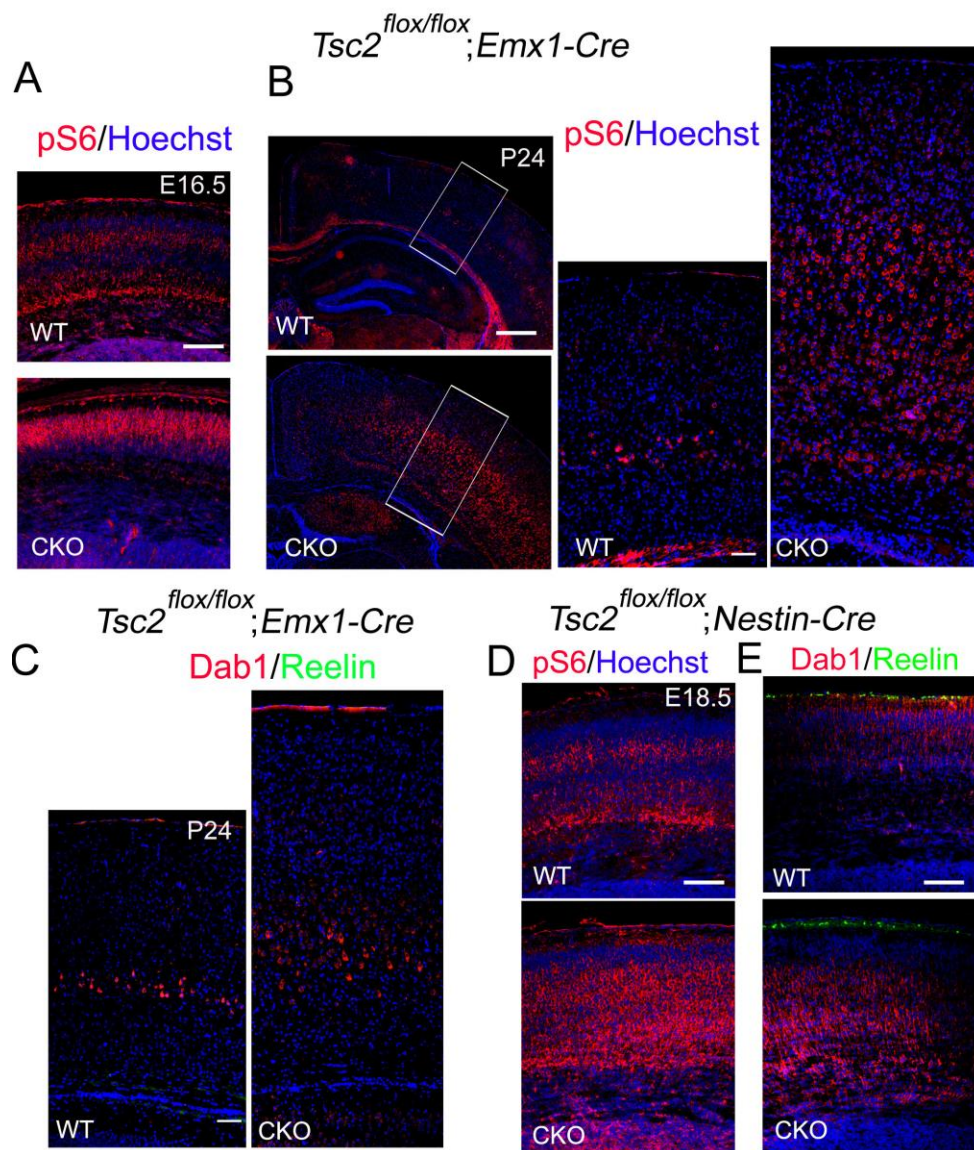


Figure S2. Reelin-Dab1 signaling is impaired in the *Tsc2* CKO mice (related to Figure 2)

(A and B) Elevated pS6 expression is detected in most cortical plate cells in CKO at E16.5 and remains high in deeper layers at P24. In WT, pS6 expression is widely detected at E16.5 but is mainly expressed in layer 5 at P24. (C) Reelin expression is completely reduced in both WT and CKO at P24, but Dab1 is slightly increased in layer 5 neurons of CKO compared to WT. (D) Increased pS6 expression in *Tsc2^{flox/flox}; Nestin-Cre* mice at E18.5. (E) Dab1 is widely distributed in the cortex of both WT and *Tsc2^{flox/flox}; Nestin-Cre* mice but markedly increased in CKO cortex. Scale bar: 200 μm (B left), 40 μm (A, B enlarged, C, D and E).

Figure S3

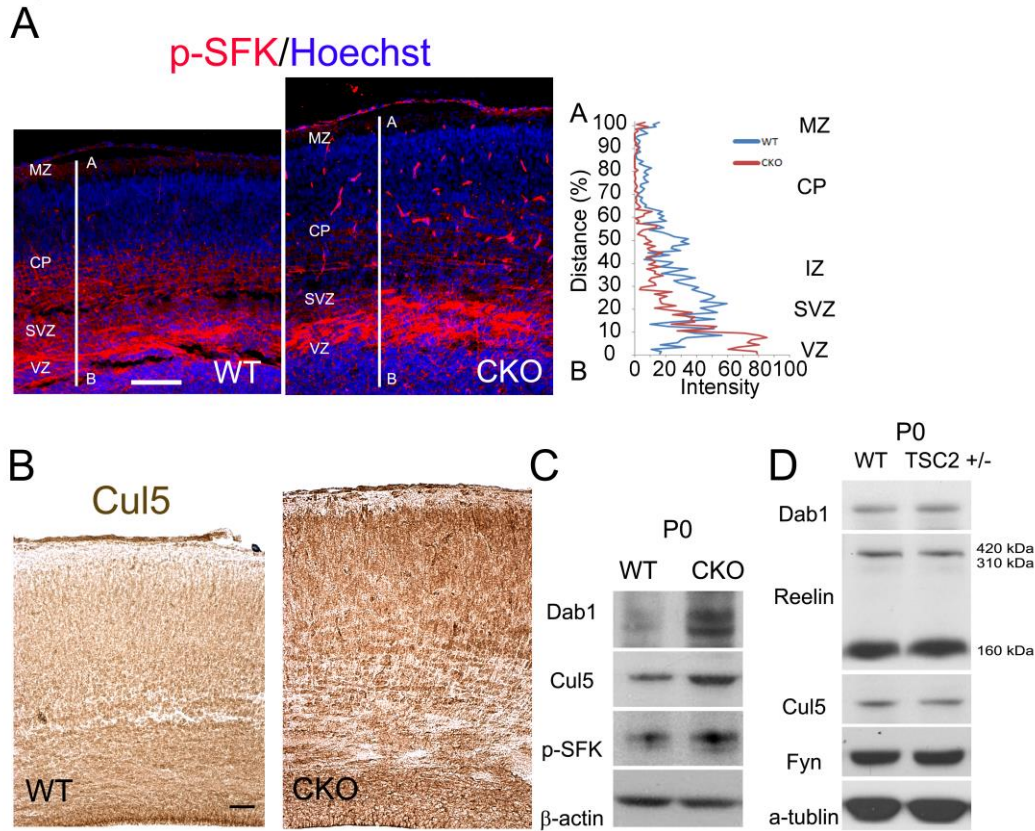


Figure S3. Upstream regulators of Reelin-Dab1 signaling are altered in *Tsc2^{flx/flx}; Nestin-Cre* mice (related to Figure 3)

(A) pSFK is expressed in the cortical plate and intensely expressed in the subventricular zone (SVZ) and ventricular zone (VZ) of WT. pSFK expression is more concentrated in the VZ and SVZ of the CKO, but expression in the cortical plate is lower. Immunostained images were further analyzed for fluorescent signal intensity with ImageJ to confirm pSFK expression area in WT and CKO cortex. (B) Immunostaining of Cul5 in the cortex demonstrates a focal increase in the upper layer of cortical plate in the CKO compared to WT. (C) Western blot shows higher Cul5, Dab1, and pSFK expression in CKO than WT. (D) Western blot does not show abnormal expression of Reelin Dab1 signaling molecules by *Tsc2* heterozygote. Scale bar: 40 μ m.

Figure S4

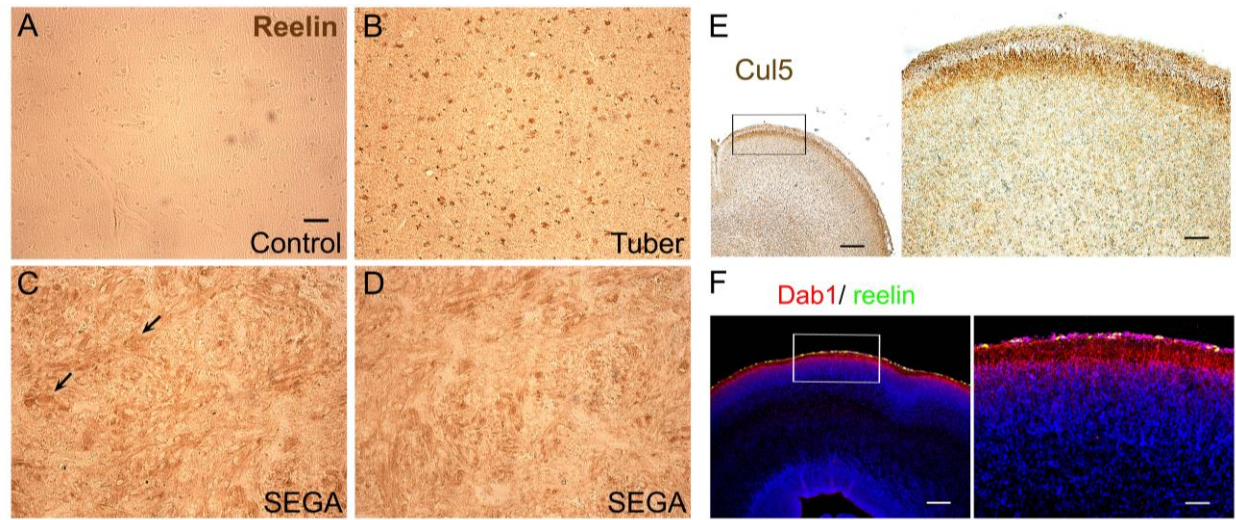


Figure S4. Reelin is highly expressed in the cortical tubers and SEGA of TSC patients (related to Figure 4)

(A-B) Reelin expression is barely detectable in control sections but intense in the cortical tuber. (C-D) Reelin expression is also abundant in large spindle shaped SEGA (subependymal giant cell astrocytoma) cells (arrows). (E) Cul5 expression is enriched in the top of the cortical plate of 19 weeks old human embryo (F) CR cells in the MZ of the human embryonic samples express Reelin (green), and cortical plate neurons show prominent expression of Dab1 (red). Scale bar: 200 μm (E left and F left), 50 μm (A-D, E right and F right).

Figure S5

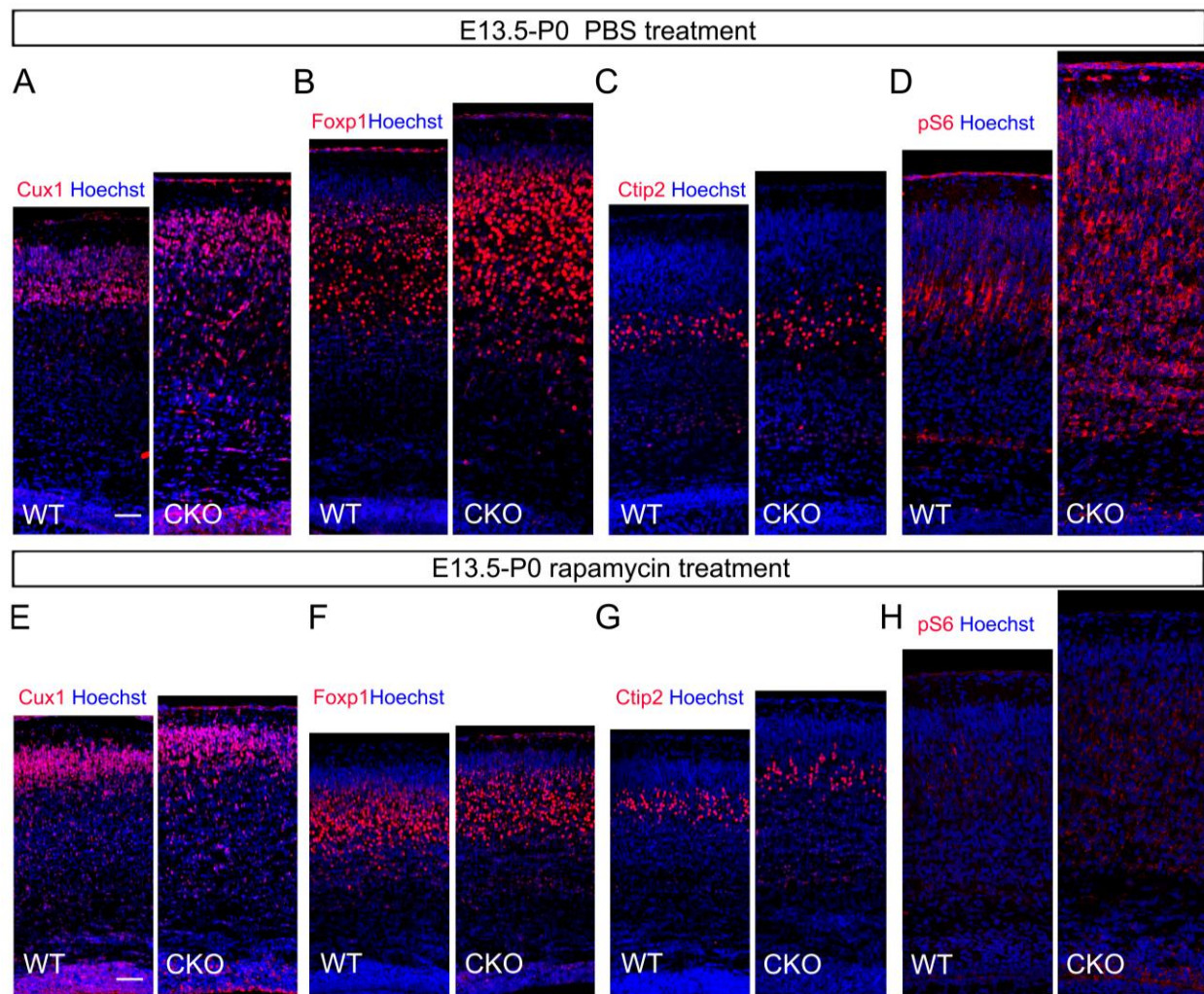


Figure S5. Rapamycin treatment rescues lamination defects of *Tsc2* CKO (related to Figure 5)

(A-H) Rapamycin treatment significantly reduces ectopic cells labeled by layer specific markers Cux1 (E), Foxp1 (F), and Ctip2 (G), compared to PBS treated controls (A, B, C), and decreases pS6 expression in both WT (D) and CKO (H). Scale bar: 20 μ m.

Figure S6

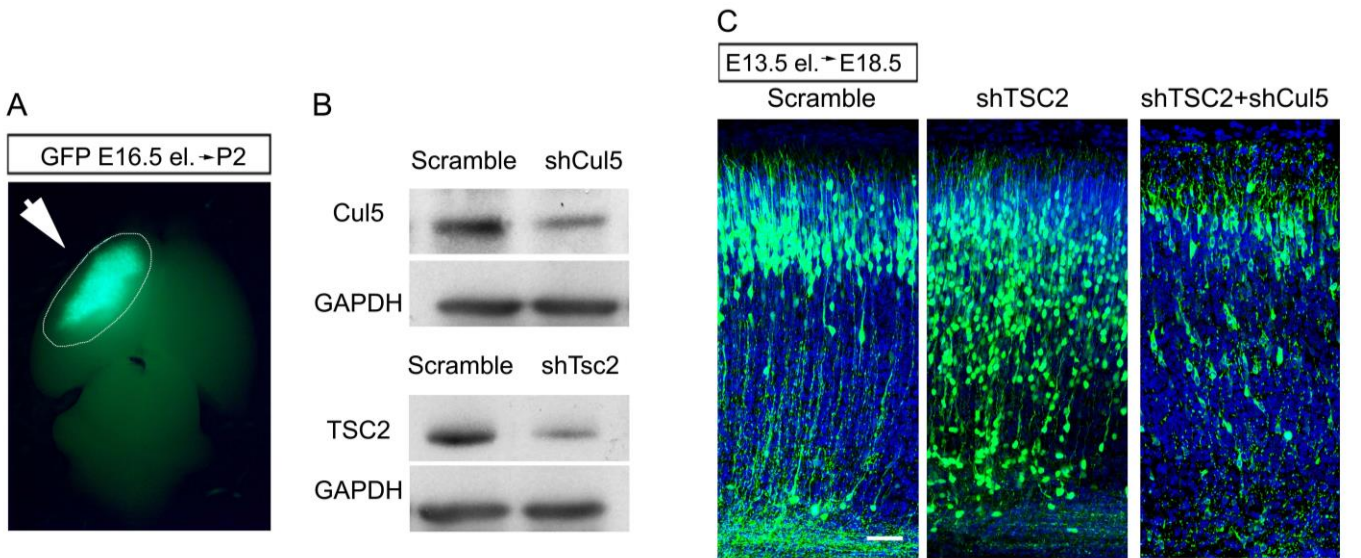


Figure S6. The efficacy of shRNA in *in utero* electroporated cortical lysates (related to Figure 6)

(A) *In utero* electroporation was performed at E16.5 to express shRNA, and the GFP-expressing region (dotted circle) was dissected at P2. (B) Western blot analyses at P2 show that *Cul5* and *Tsc2* knockdown constructs decrease *Cul5* and *Tsc2* expression after *in utero* electroporation at E16.5 (C) shRNA constructs for *Tsc2* and *Cul5* or *Tsc2* and control (Scrambled) were electroporated at E13.5, and neuronal migration defects were analyzed at E18.5. Scale bar: 40 μm.

Figure S7

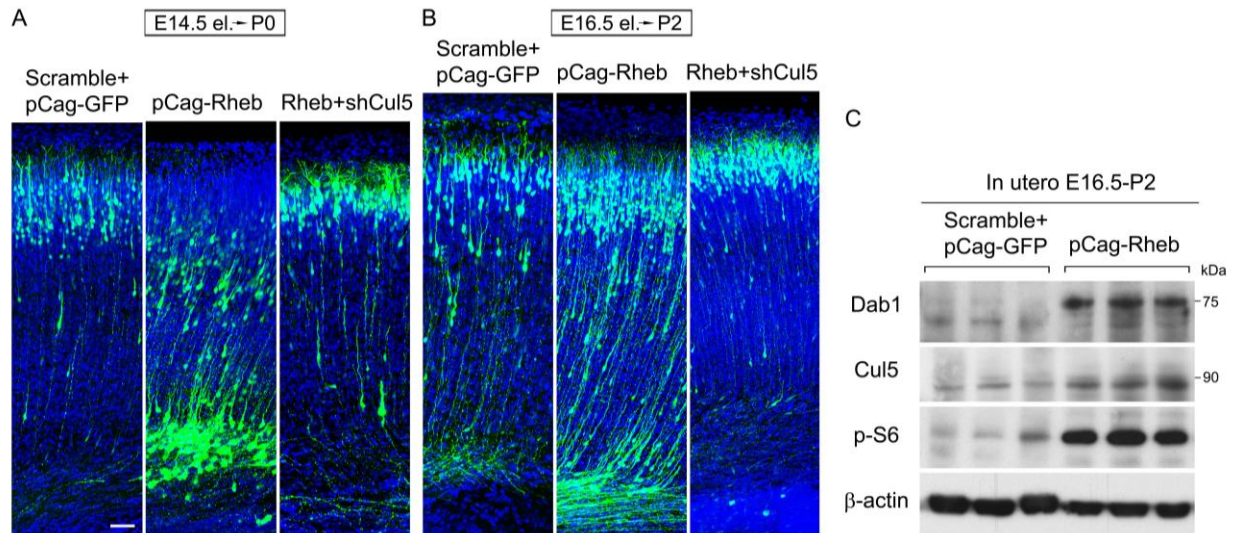


Figure S7. Rheb overexpression impairs neuronal migration and Reelin-Dab1 signaling by enhancing Cul5 expression (related to Figure 7)

(A and B) Rheb constructs, scrambled shRNA control only or along with *Cul5* shRNA, were electroporated at E14.5 and E16.5. (C) Western blots for Dab1, Cul5 and pS6 show that Rheb expression increases protein levels in the electroporated cortices. Scale bar: 40 μ m.

(B) Western blot analyses of pCAG-Rheb electroporated cortical areas reveal increased Cul5 and Dab1 protein levels compared to control construct-electroporated areas.